Precise short- and long-term propagation of orbits and uncertainties using the Hermite integration scheme for LEO space debris objects

J. Rodmann, D. Hampf, T. Hasenohr, L. Humbert, W. Riede, F. Sproll, P. Wagner

German Aerospace Center (DLR)

Institute of Technical Physics, Stuttgart, Germany

Outline

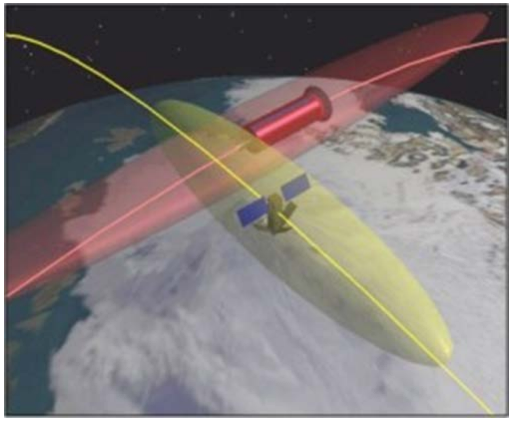

Motivation

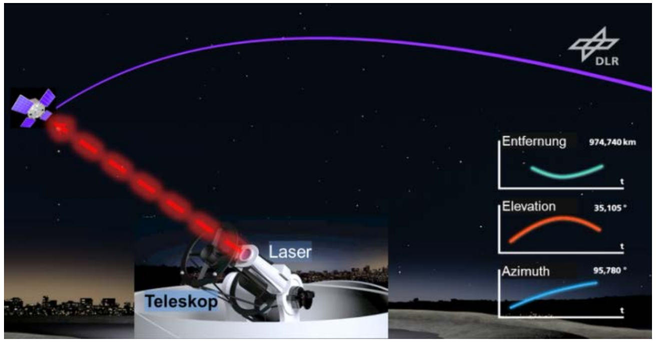

Debris laser ranging

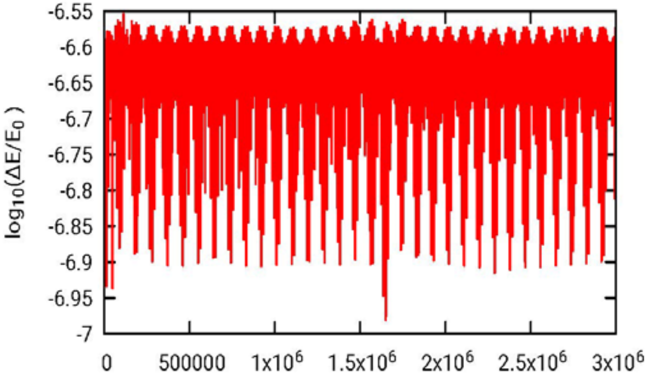

Hermite integration

Space debris is a growing threat to the safe and cost-effective operation of space systems

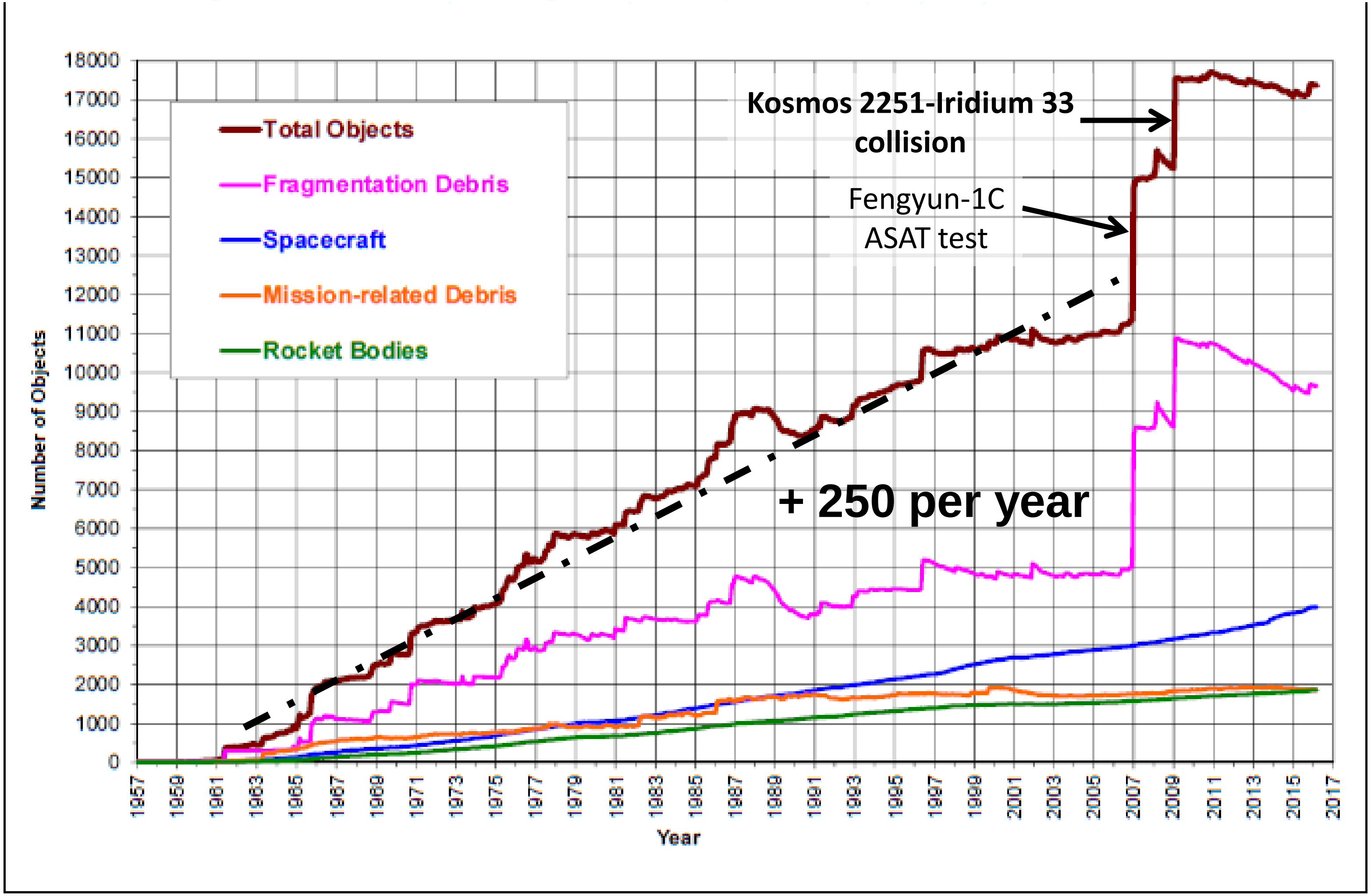

© NASA
Orbital Debris Quarterly News
Vol 20, 2016

The Iridium 33–Cosmos 2251 collision highlighted the importance of actionable orbit uncertainties

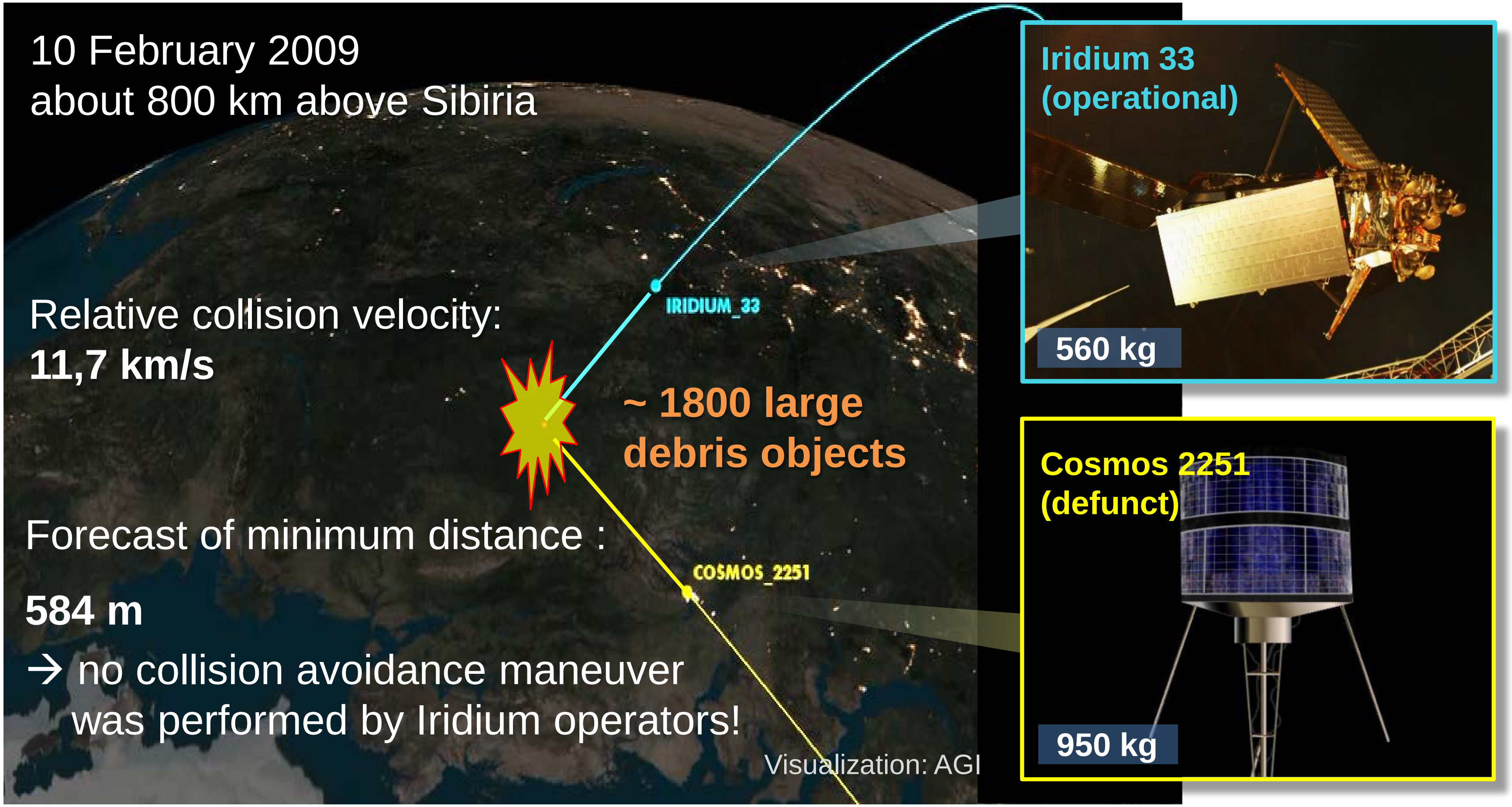

10 February 2009
about 800 km above Sibiria

Relative collision velocity:
11,7 km/s

~ 1800 large debris objects

Forecast of minimum distance :

584 m

→ no collision avoidance maneuver was performed by Iridium operators!

Iridium 33 (operational)

560 kg

Cosmos 2251 (defunct)

950 kg

Visualization: AGI

Space debris objects of about 10 cm size and larger are detected and tracked by radar and optical telescopes

Tracking radar for LEO objects

Passive-optical tracking for GEO objects

Passiv-optical imaging of LEO satellites

TLE data have inherent uncertainties in the km range, limiting their usage for effective conjunction analyses

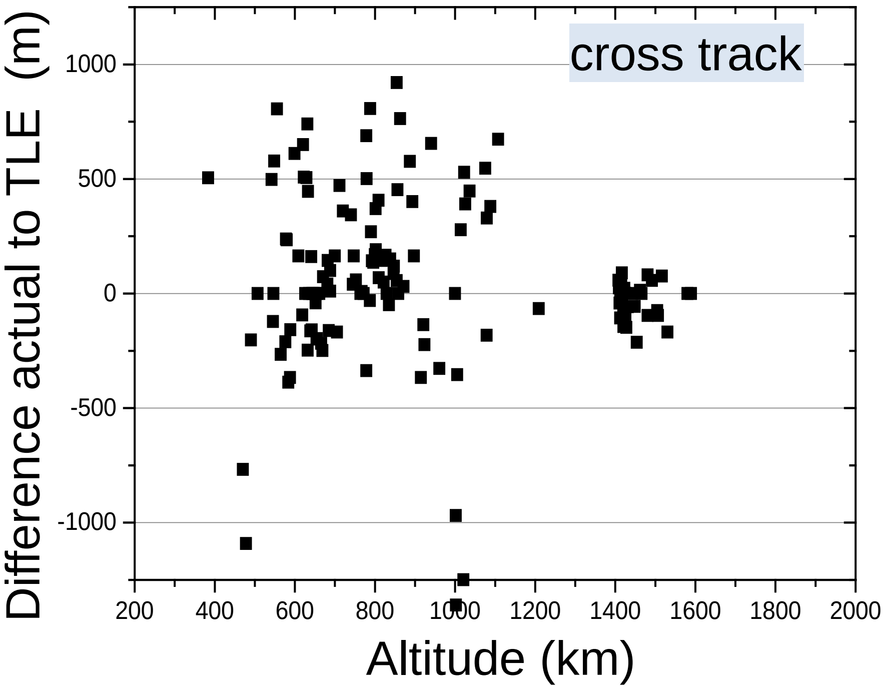

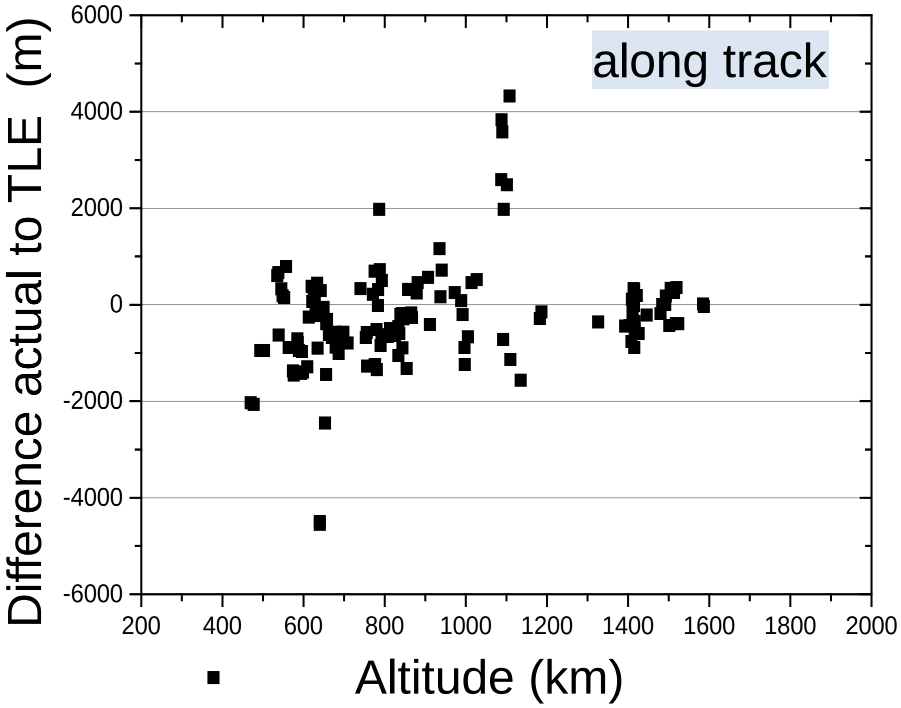

59 objects / 150 passes
Analysis: G. Kirchner, Graz

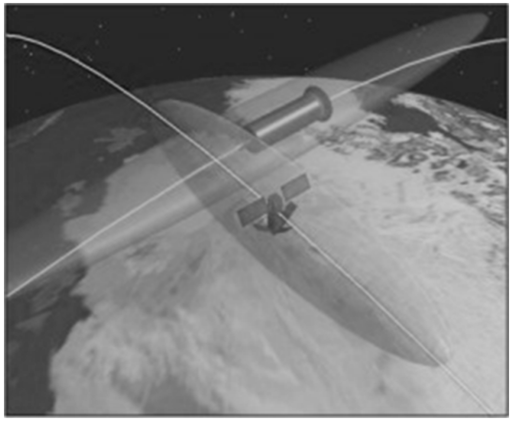

Motivation

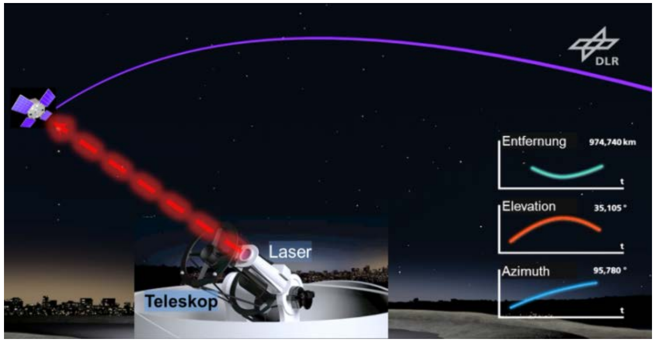

Debris laser ranging

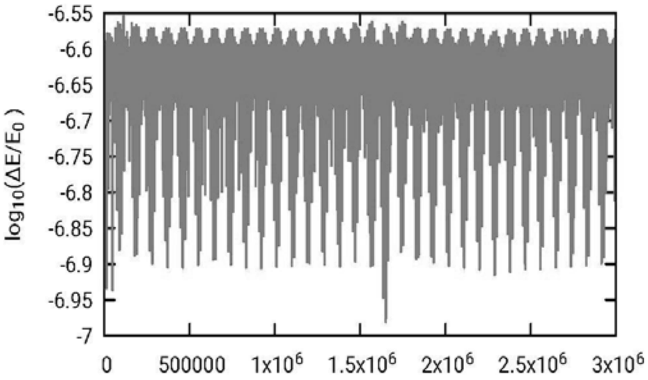

Hermite integration

Laser ranging and tracking can be used to determine precise distance and angles of space debris objects

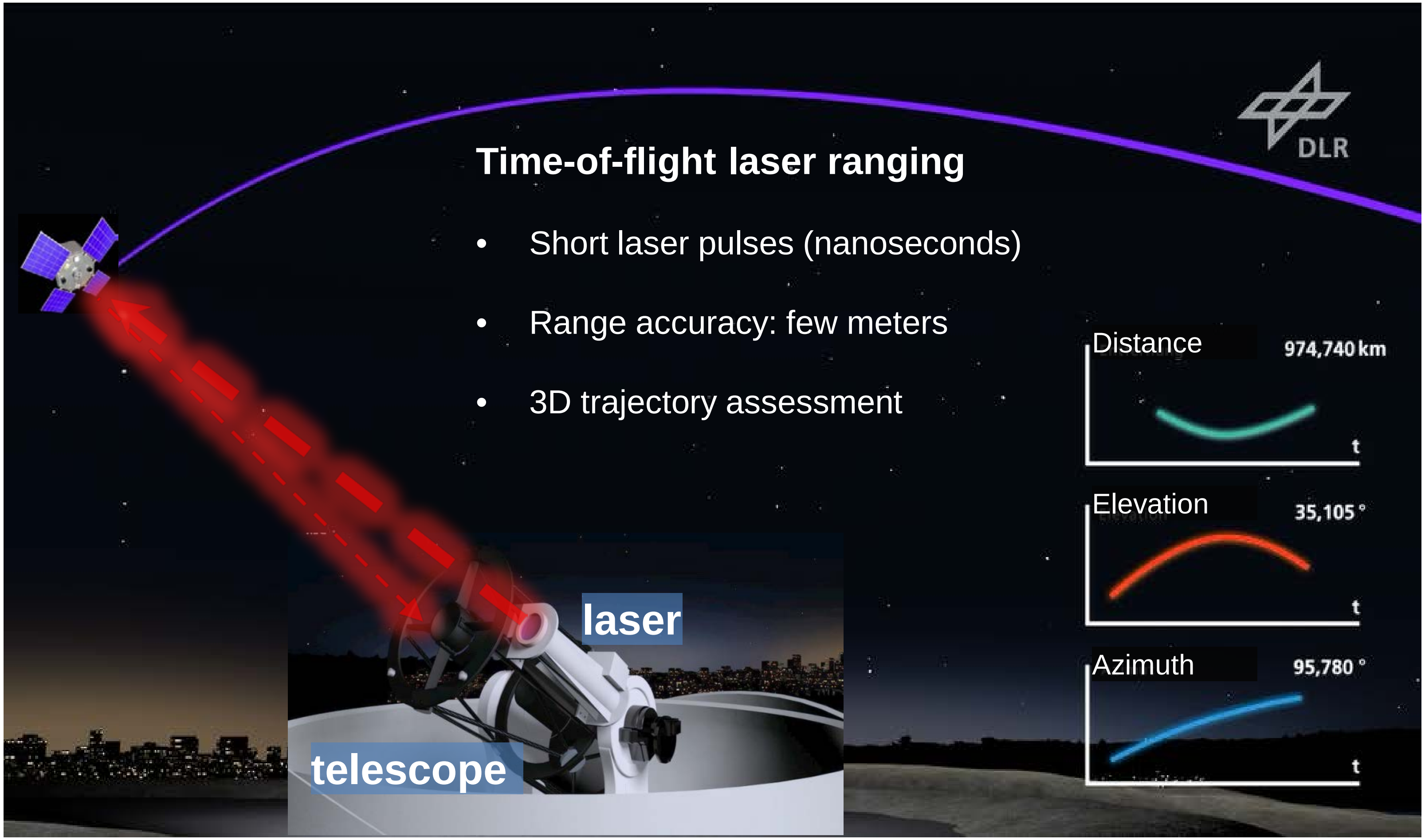

Time-of-flight laser ranging

- Short laser pulses (nanoseconds)
- Range accuracy: few meters
- 3D trajectory assessment

Laser ranging to cooperative targets, i.e. equipped with retro-reflectors routinely provides sub-metre precision

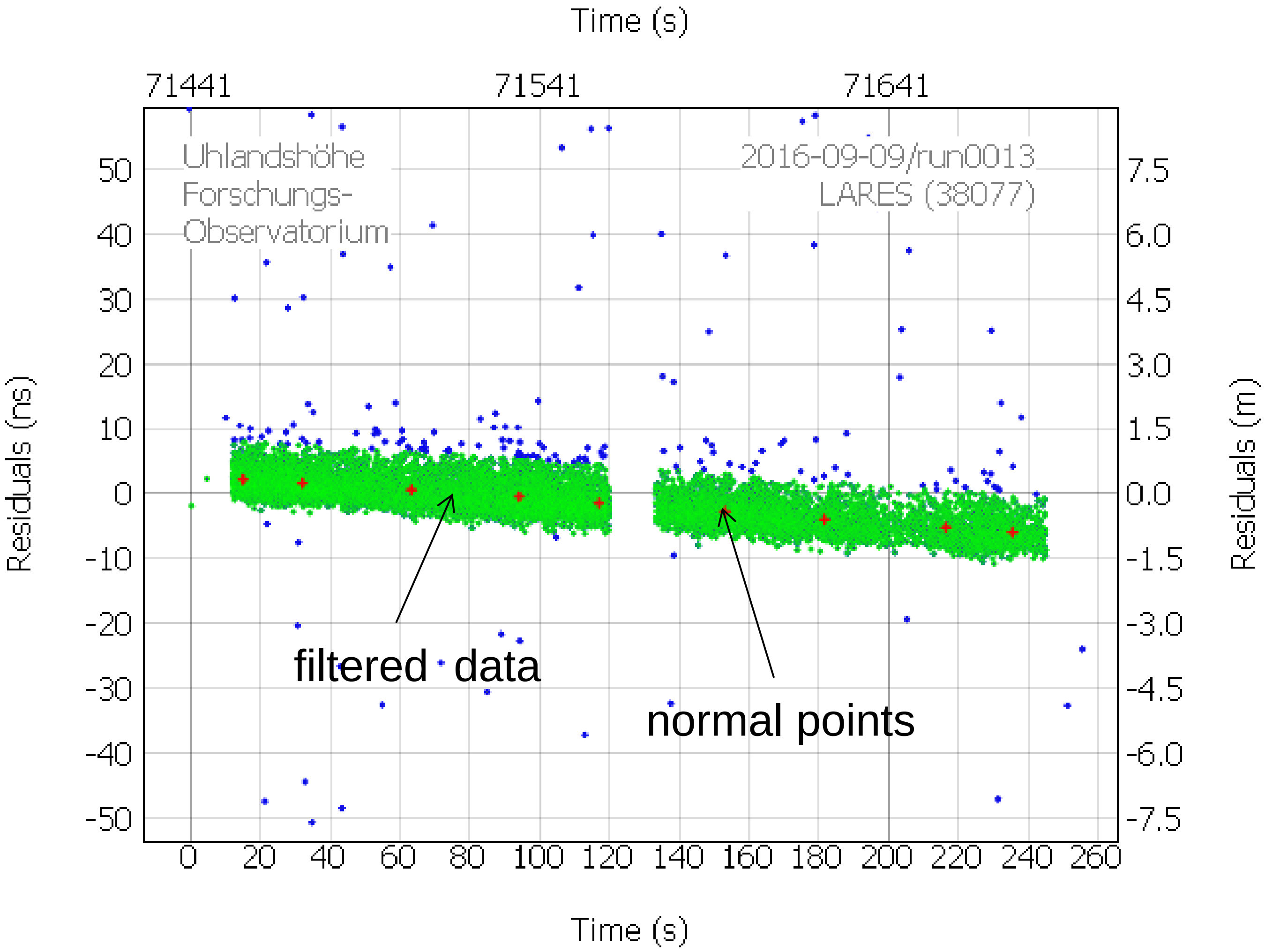

filtered data

normal points

Satellite Laser Ranging vs. Space Debris Laser Ranging

	Satellite Laser Ranging (SLR)	Space Debris Laser Ranging (SDLR)
Application	Geodesy	Orbit Determination
Achieved in	~ 1964	~ 2004
Operational stations	approx. 40	1 – 2
Experimental stations	approx. 5	approx. 5
Targets	approx. 100 (cooperative)	> 10 000 (non-cooperative)
Precision	< 1 cm	~ 1 m
Pulse energy	ca. 100 µJ – 1 mJ	> 100 mJ
Data analysis	8 analysis centres	individually
Organization	International Laser Ranging Service	—

Fusion of laser ranges and pseudo angular (TLE) data reduces the predicted orbit uncertainty

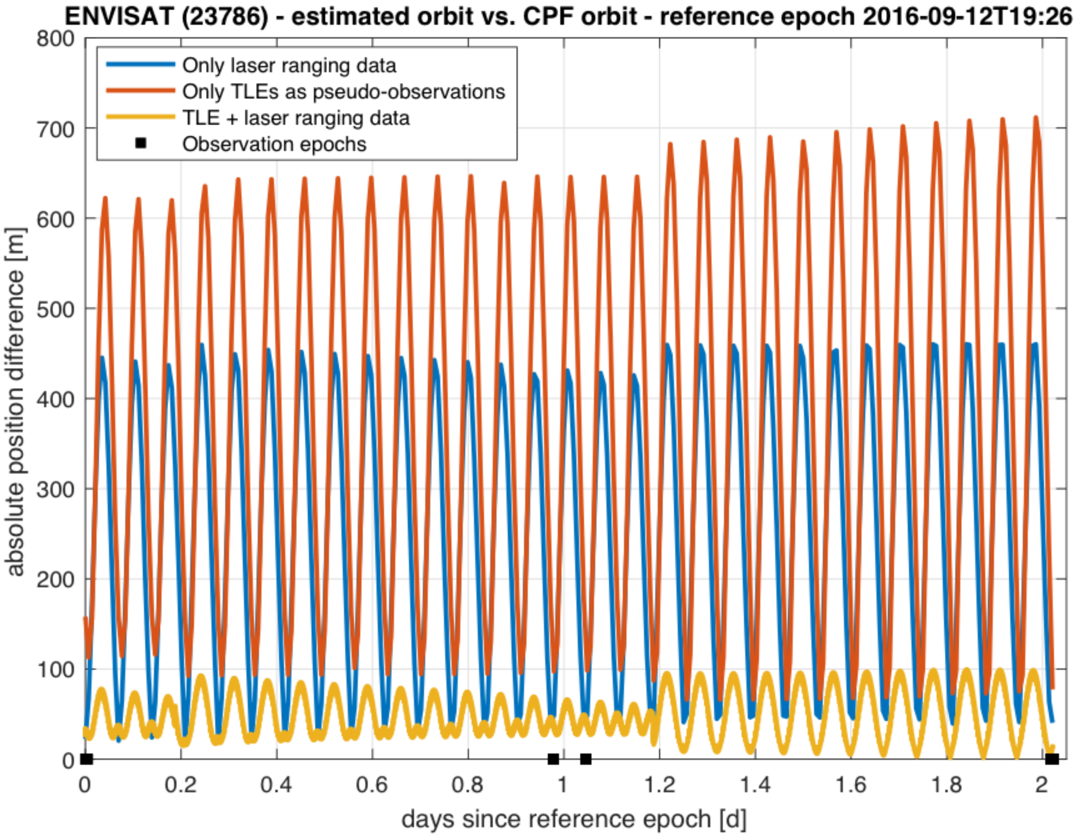

Comparison with concatenated 1-day CPF predictions

Weighting of TLE pseudo-data to laser measurements 1:10

ESA GSTP activity
“Accurate orbit determination of space debris with laser ranging/tasking”
Chr. Bamann, TU Munich, Germany

We are developing laser ranging and tracking hardware and software, mainly geared towards LEO space objects

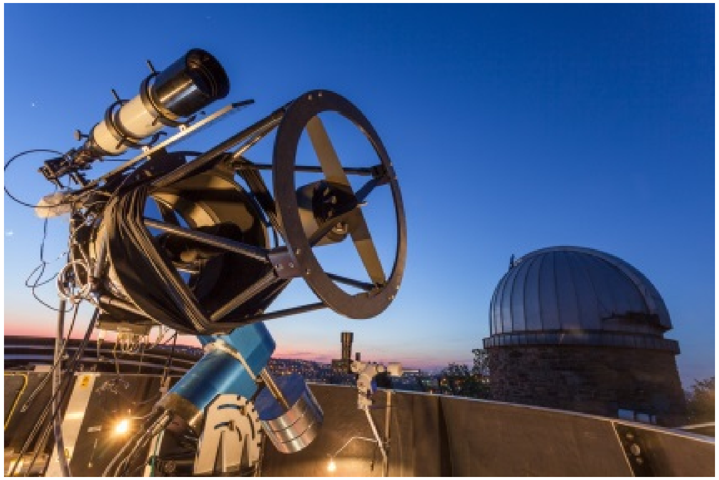

Uhlandshöhe Forschungsobservatorium (UFO)

SLR ground station testbed
- 10-cm laser telescope, fibre-fed
- 43-cm receiver telescope
- equatorial mount

Surveillance Tracking and Ranging Container (STaR-C)

Transportable Debris Laser Ranging Station
- 10-cm laser telescope
- Same receiver telescope as UFO
- Laser path through axes of alt-az mount

Selection of observing sites considered for transportable laser ranging station

Andøya Space Center
Andøya, Norway

Auger Observatory
Malargüe, Argentina

GARS-O’Higgins
Kap Legoupil, Antarctica

Observatorio del Teide
Tenerife, Spain

Southern African Large Telescope (SALT)
Sutherland, South Africa

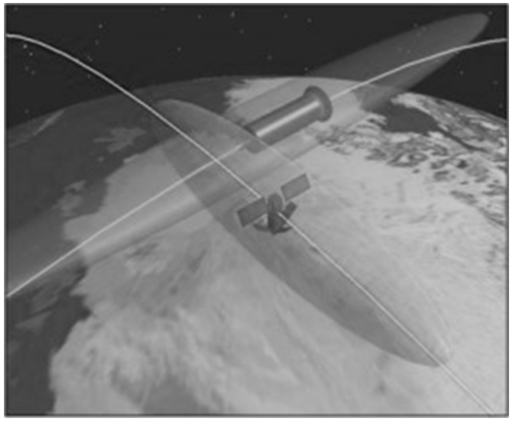

Motivation

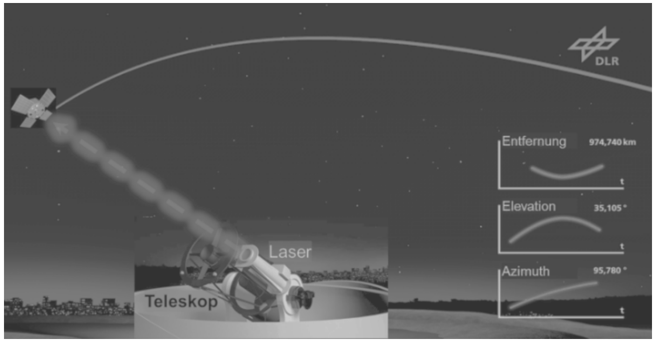

Debris laser ranging

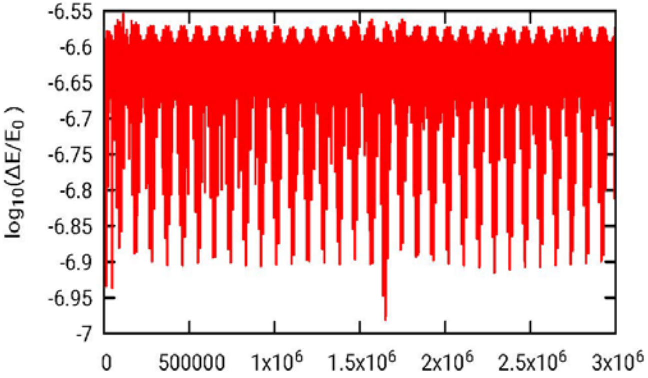

Hermite integration

We require an accurate, versatile, and fast integration method for propagating orbits and uncertainties

Accurate → conserving first integrals (energy, angular momentum)
Versatile → applicable for all orbit types and integration times
Fast → capable of integrating many objects simultaneously

Hermite integration scheme

- Direct numerical integration method using Cartesian coordinates
- Widely used in the astronomical N-body community (Makino 1991, Makino & Aarseth 1992, Kokubo & Makino 2004)

- Needs acceleration $\boldsymbol{a}$ and its first derivative $\mathrm{d}\boldsymbol{a}/\mathrm{d}t$
- Second and third derivatives can be calculated based on $\boldsymbol{a}$ and $\boldsymbol{a}/\mathrm{d}t$ alone

- For constant timesteps the Hermite integrator is time-symmetric
- No secular errors in semi-major axis and eccentricity but small drift in ω

Test cases (Hull et al. 1972): Comparison of state vectors after 20/2π or about 3.2 orbits

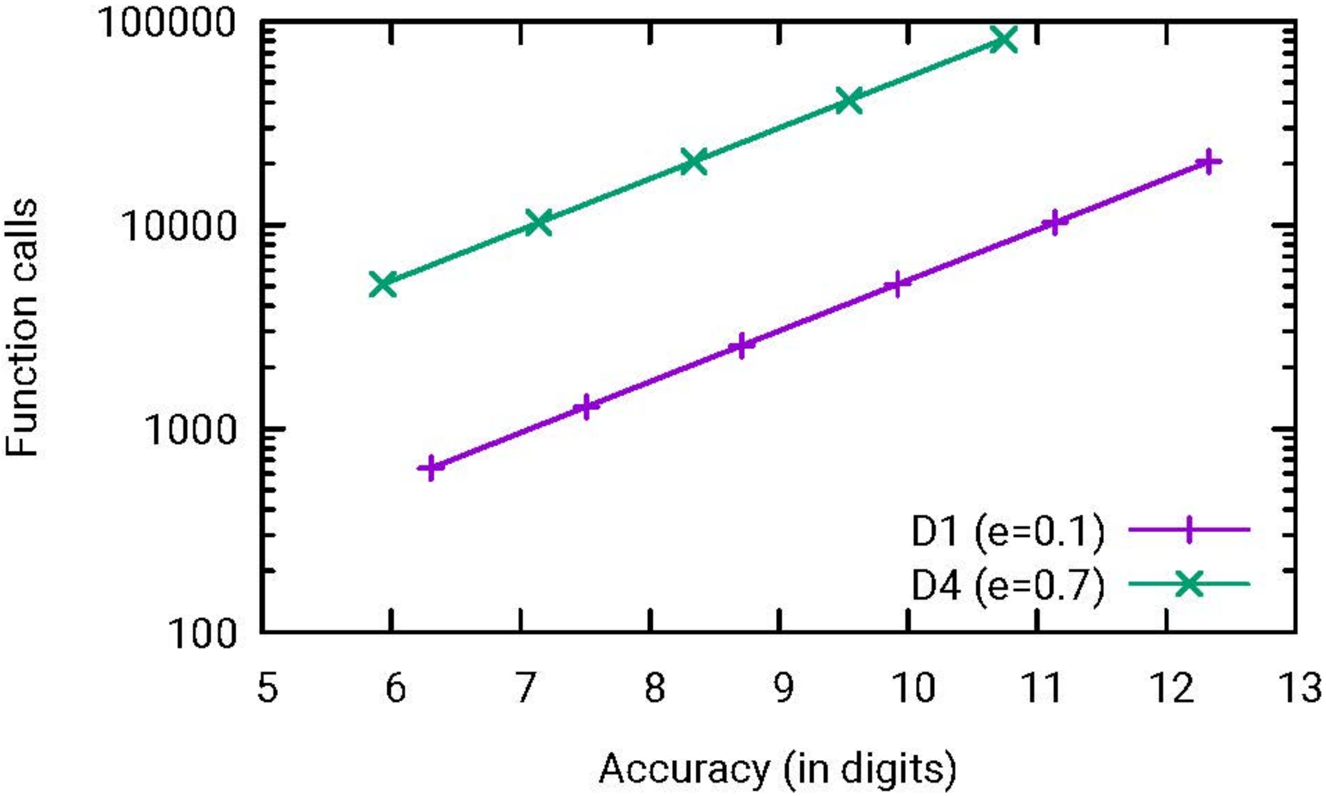

Numerical accuracy defined as

$$\varepsilon = -\log\sqrt{\sum_{k=1}^{4}(x_k - \hat{x}_k)^2}$$

Short-term integration:
100 orbits, corresponds to ~7 days for 100-min orbit

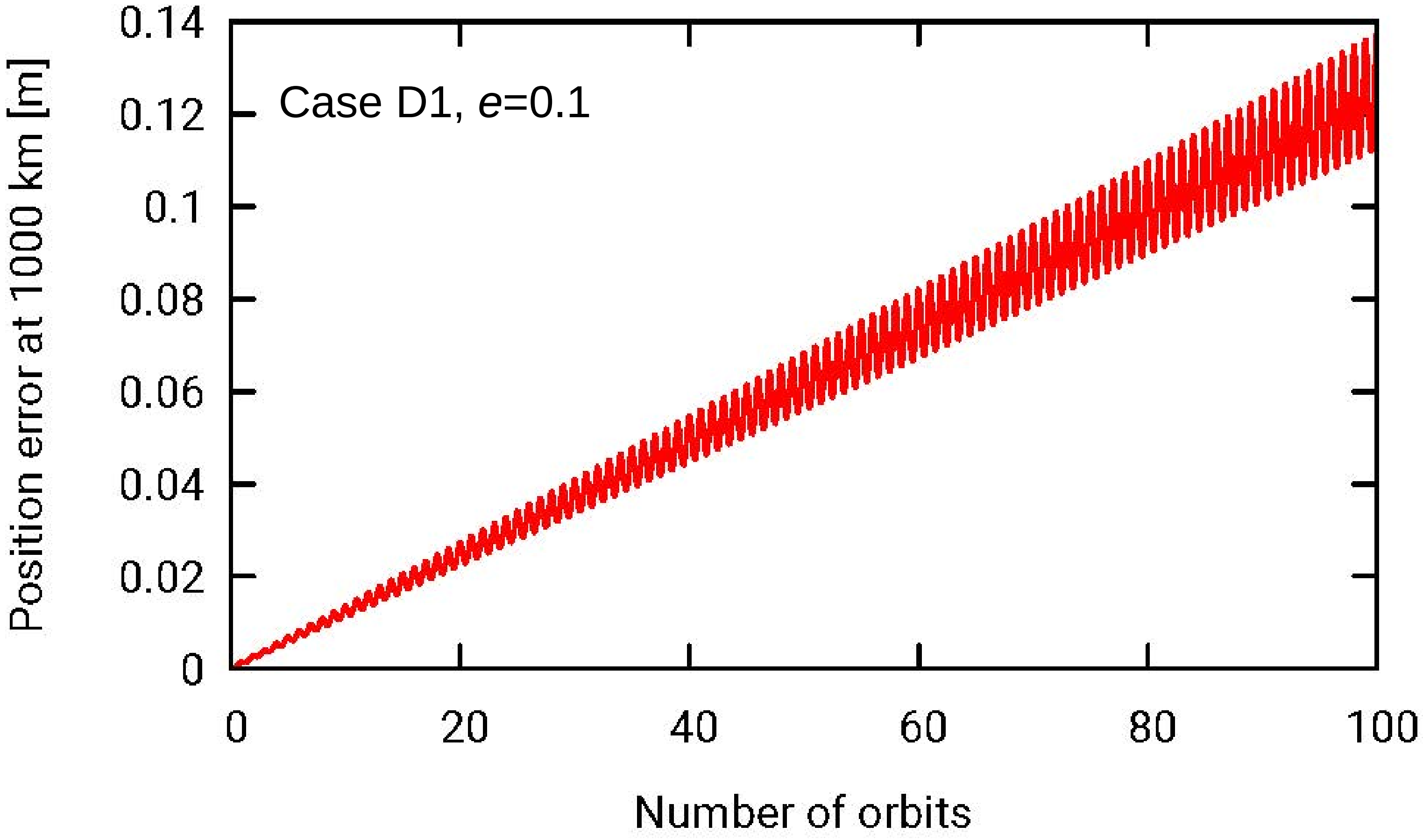

Short-term integration:
100 orbits, corresponds to ~7 days for 100-min orbit

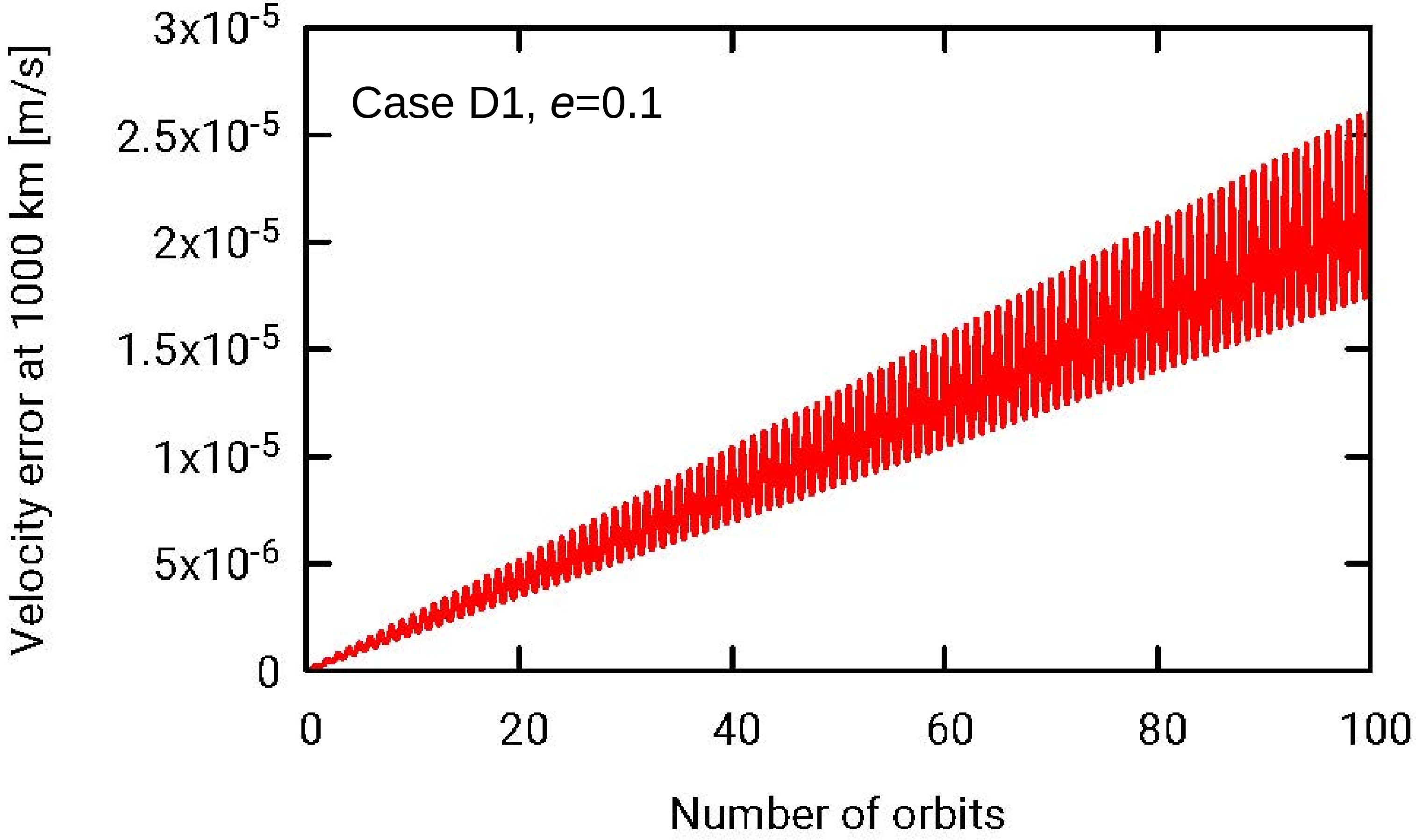

Long-term integration:
3.2 million orbits, corresponds to ~600 yrs for LEO orbit

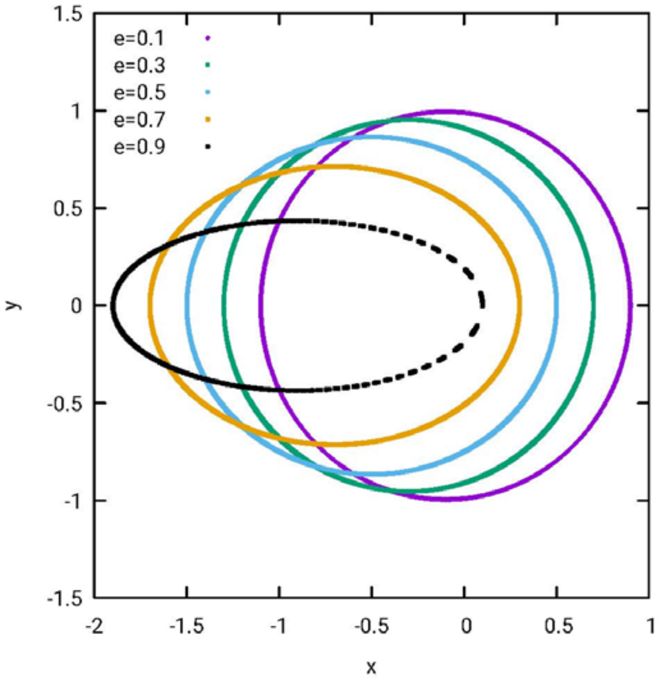

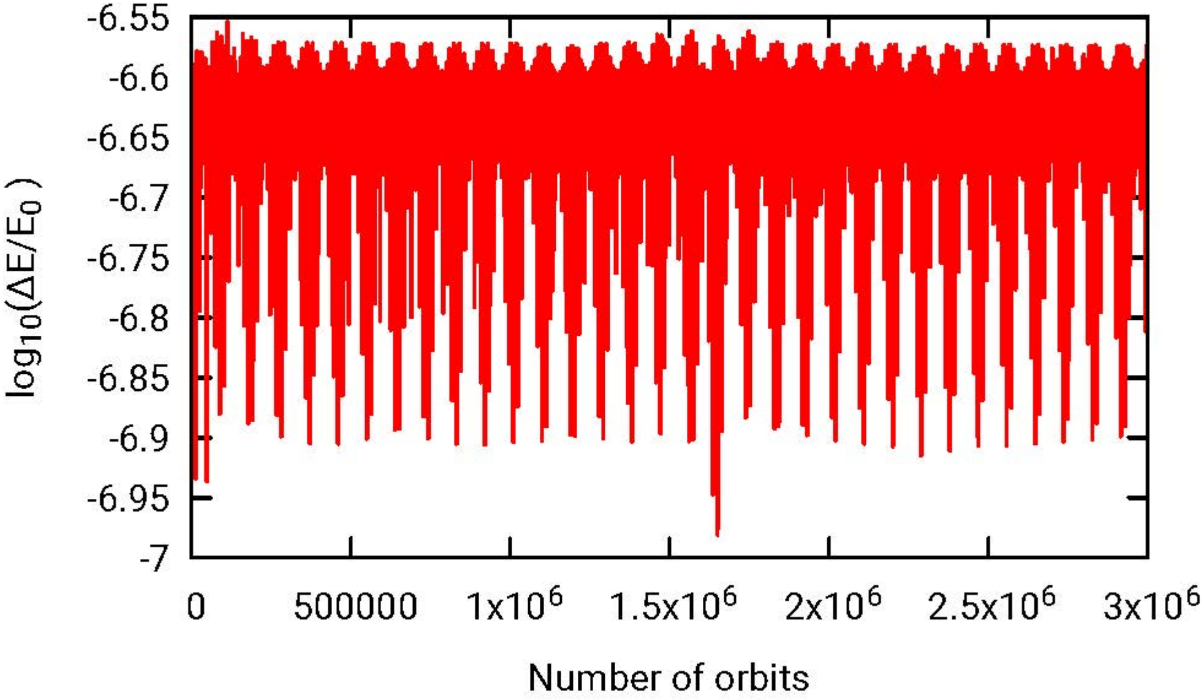

Long-term integration:
3.2 million orbits, corresponds to ~600 yrs for LEO orbit

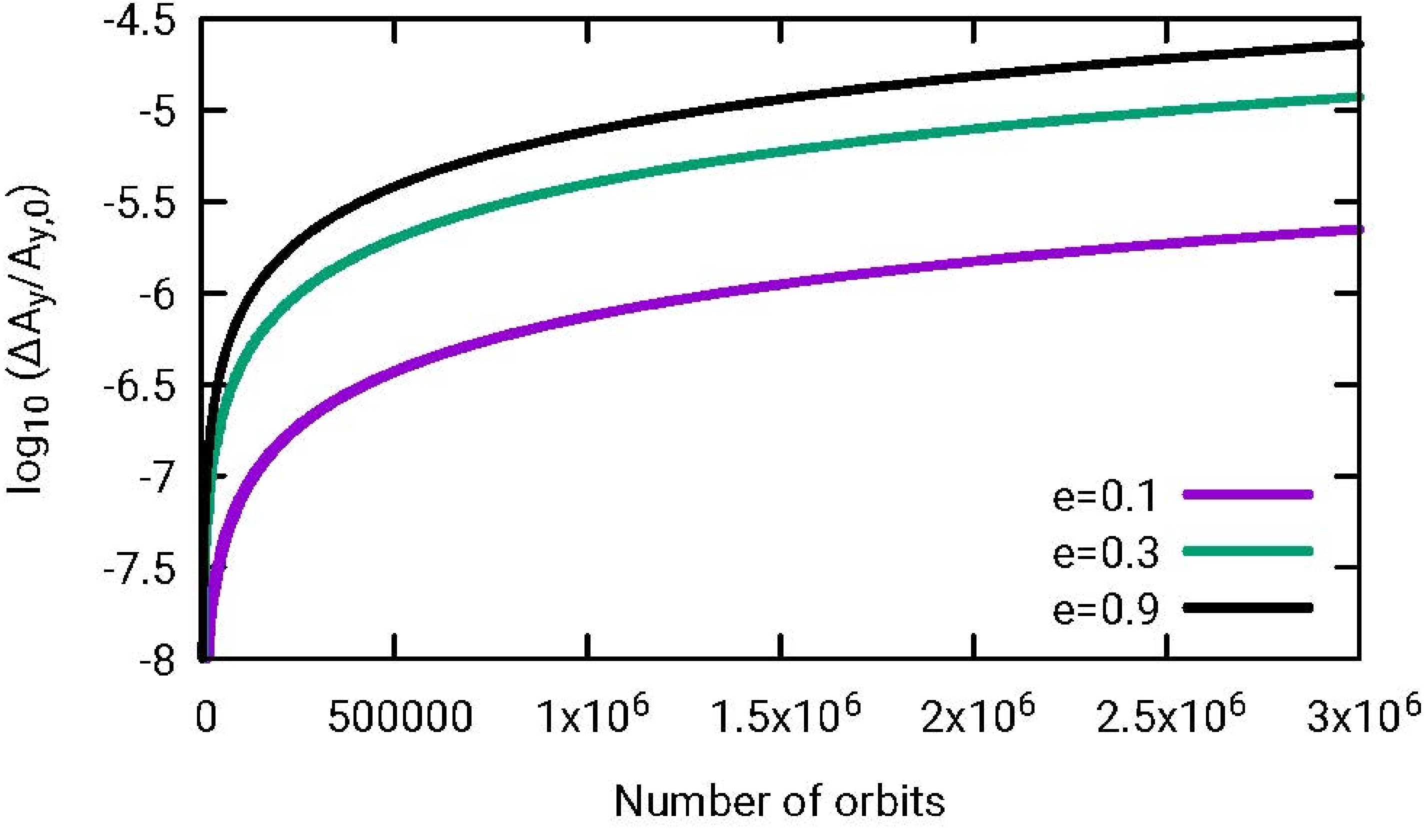

Summary and outlook

- Realistic and actionable uncertainties are important for many SSA applications
- Laser ranging to space debris objects promises order of magnitude improvement
- DLR is developing hardware for testing the technology that could be part of a sensor network
- The Hermite scheme is an attractive integration method because it has no secular errors in semi-major axis and eccentricity

Next steps

- Implementation of force model (Earth potential, 3rd body, SRP, drag)
- Detailed comparison of results with other propagation methods and codes
- Analysis and optimization of a global network of debris laser ranging stations

Backup slides

Measurements: Residual Plots

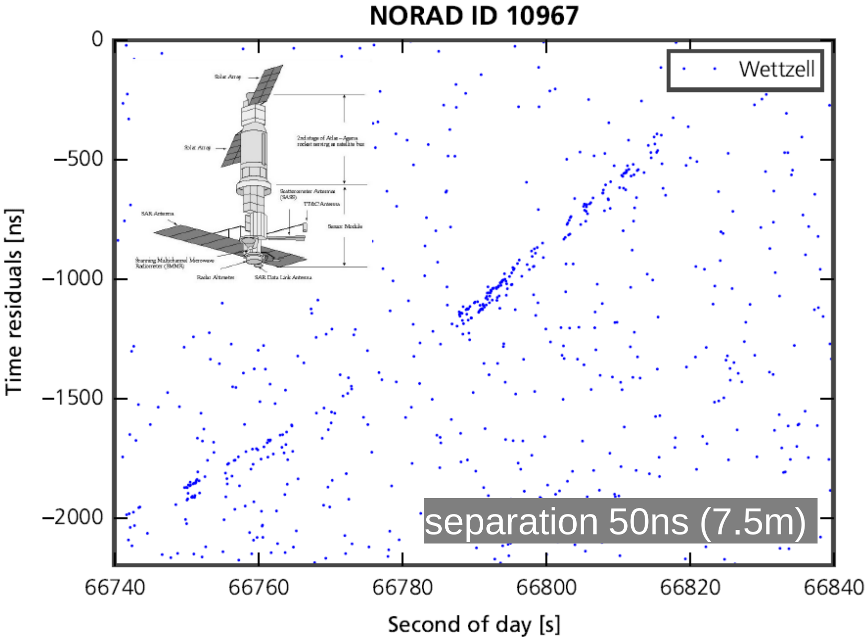

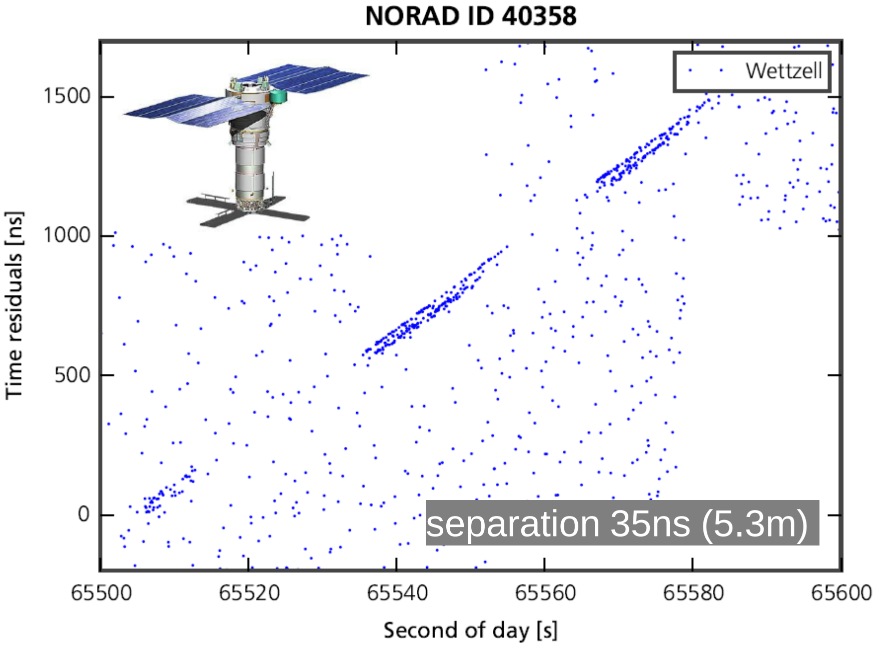

- laser ranging data can provide information about **structure** and **dimension** of objects

Measurements: Residual Plots

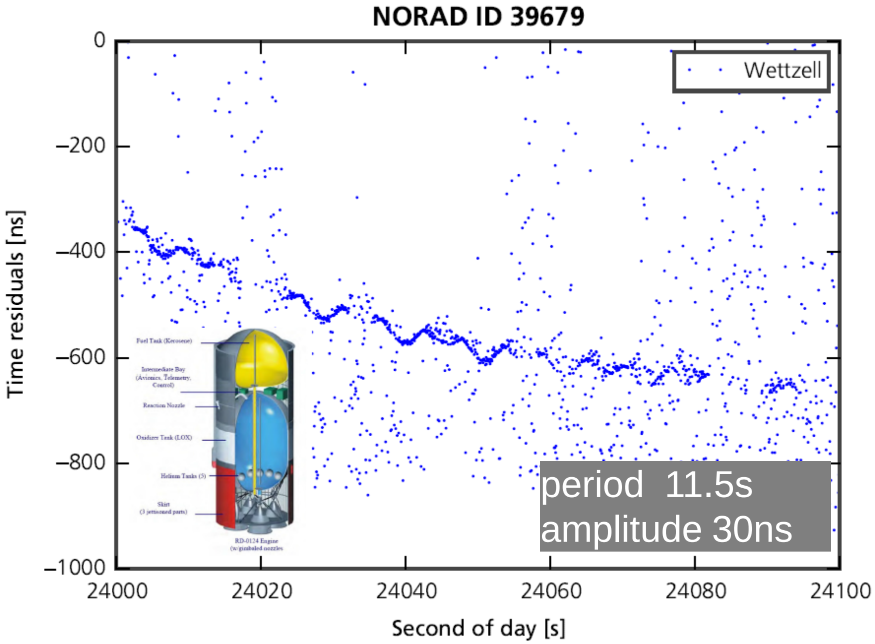

period 11.5s
amplitude 30ns

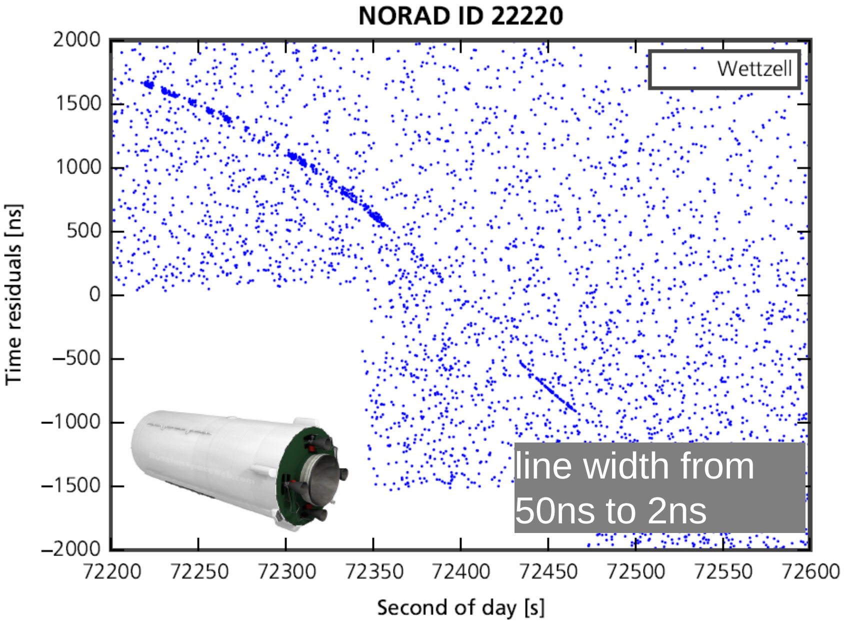

line width from
50ns to 2ns

- laser ranging data can provide information about **rotational behavior** and **dimension** of objects

Modelling of Orbital Debris and Artificial Satellite Trajectories (MODAST)

- Numerical propagator based on the Hermite integration scheme
  - Previously for dynamical modelling of circumstellar dust (Rodmann 2006)
  - Iterated Predict-Evaluate-Correct method P(EC)^n

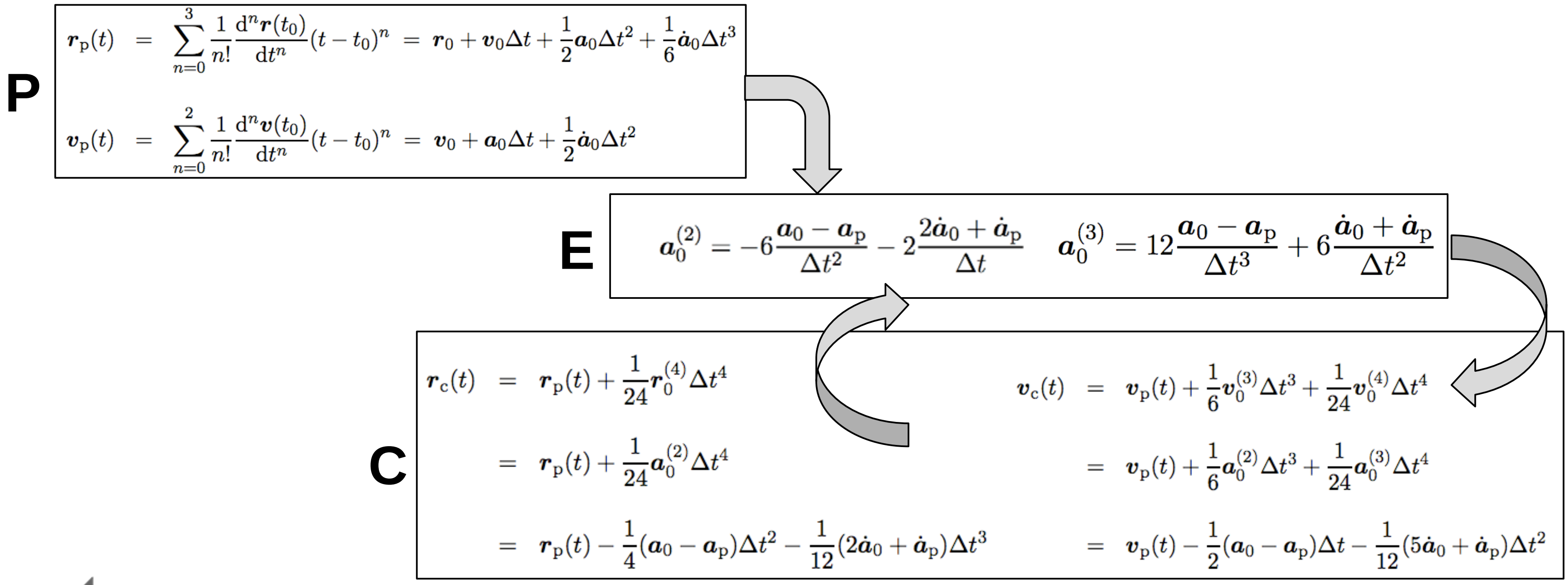

P

$$\boldsymbol{r}_\mathrm{p}(t) = \sum_{n=0}^{3} \frac{1}{n!}\frac{\mathrm{d}^n \boldsymbol{r}(t_0)}{\mathrm{d}t^n}(t-t_0)^n = \boldsymbol{r}_0 + \boldsymbol{v}_0 \Delta t + \frac{1}{2}\boldsymbol{a}_0 \Delta t^2 + \frac{1}{6}\dot{\boldsymbol{a}}_0 \Delta t^3$$

$$\boldsymbol{v}_\mathrm{p}(t) = \sum_{n=0}^{2} \frac{1}{n!}\frac{\mathrm{d}^n \boldsymbol{v}(t_0)}{\mathrm{d}t^n}(t-t_0)^n = \boldsymbol{v}_0 + \boldsymbol{a}_0 \Delta t + \frac{1}{2}\dot{\boldsymbol{a}}_0 \Delta t^2$$

E

$$\boldsymbol{a}_0^{(2)} = -6\frac{\boldsymbol{a}_0 - \boldsymbol{a}_\mathrm{p}}{\Delta t^2} - 2\frac{2\dot{\boldsymbol{a}}_0 + \dot{\boldsymbol{a}}_\mathrm{p}}{\Delta t} \qquad \boldsymbol{a}_0^{(3)} = 12\frac{\boldsymbol{a}_0 - \boldsymbol{a}_\mathrm{p}}{\Delta t^3} + 6\frac{\dot{\boldsymbol{a}}_0 + \dot{\boldsymbol{a}}_\mathrm{p}}{\Delta t^2}$$

C

$$\begin{aligned}
\boldsymbol{r}_\mathrm{c}(t) &= \boldsymbol{r}_\mathrm{p}(t) + \frac{1}{24}\boldsymbol{r}_0^{(4)}\Delta t^4 \\
&= \boldsymbol{r}_\mathrm{p}(t) + \frac{1}{24}\boldsymbol{a}_0^{(2)}\Delta t^4 \\
&= \boldsymbol{r}_\mathrm{p}(t) - \frac{1}{4}(\boldsymbol{a}_0 - \boldsymbol{a}_\mathrm{p})\Delta t^2 - \frac{1}{12}(2\dot{\boldsymbol{a}}_0 + \dot{\boldsymbol{a}}_\mathrm{p})\Delta t^3
\end{aligned}$$

$$\begin{aligned}
\boldsymbol{v}_\mathrm{c}(t) &= \boldsymbol{v}_\mathrm{p}(t) + \frac{1}{6}\boldsymbol{v}_0^{(3)}\Delta t^3 + \frac{1}{24}\boldsymbol{v}_0^{(4)}\Delta t^4 \\
&= \boldsymbol{v}_\mathrm{p}(t) + \frac{1}{6}\boldsymbol{a}_0^{(2)}\Delta t^3 + \frac{1}{24}\boldsymbol{a}_0^{(3)}\Delta t^4 \\
&= \boldsymbol{v}_\mathrm{p}(t) - \frac{1}{2}(\boldsymbol{a}_0 - \boldsymbol{a}_\mathrm{p})\Delta t - \frac{1}{12}(5\dot{\boldsymbol{a}}_0 + \dot{\boldsymbol{a}}_\mathrm{p})\Delta t^2
\end{aligned}$$